Analyst

ROYAL SOCIETY OF CHEMISTRY

PAPER

View Article Online
View Journal | View Issue

Cite this: *Analyst*, 2024, **149**, 4932

Paper-based analytical device for point-of-care nucleic acid quantification combining CRISPR/Cas12a and a personal glucose meter†

Yohei Tanifuji, Guodong Tong, Yuki Hiruta and Daniel Citterio *

Although CRISPR-based nucleic acid detection has great potential in point-of-care testing due to its simplicity, it has been rarely integrated into paper-based analytical devices (PADs), which are attractive platforms to simplify assays. This work introduces a CRISPR-assisted nucleic acid quantification approach integrated into a PAD with signal readout by a personal glucose meter (PGM). Retention of magnetic beads by filter paper and pre-deposition of all required reagents by freeze-drying stabilized with trehalose enabled the indirect quantification of human papilloma virus (HPV) DNA through a PGM readout without complicated user intervention and complex reagent handling. The calculated limit of detection was 57 pM, which is comparable with other amplification-free CRISPR-based assays detecting nucleic acids. The fully integrated device exhibited good storage stability for up to 4 weeks, suggesting its applicability toward practical point-of-care nucleic acid quantification.

Received 27th June 2024,
Accepted 27th July 2024

DOI: 10.1039/d4an00905c

rsc.li/analyst

Introduction

Since the first report of a nucleic acid detection method assisted by the clustered regularly interspaced short palindromic repeats (CRISPR)/CRISPR-associated protein (Cas)12a system, this assay technology has been drawing great attention for its sensitivity, single-base specificity and simplicity.[1,2] It is notable that the flexible design of CRISPR RNA (crRNA) in combination with Cas12a proteins enables recognition of any complemental dsDNA carrying a specific sequence called a protospacer adjacent motif (PAM). Following this recognition step, the Cas12a-crRNA-dsDNA assembly exhibits collateral nuclease activity referred to as trans-cleavage, indiscriminately cleaving surrounding ssDNA, even at room temperature.[1,3,4] Hence, an abundant number of point-of-care CRISPR-based assays has been reported with colorimetric[5–8] and fluorescence[9–12] signal detection. However, in terms of user-friendliness, there are remaining challenges for point-of-care testing (POCT), since the previously reported assays require multiple steps of operation involving reagent handling, pipetting and separation, among others.

In contrast, paper-based analytical devices (PADs) have become attractive platforms to achieve POCT, due to their low cost, ease of operation, disposability, and simplicity.[13,14] Taking into account these benefits, some researchers have combined CRISPR-based assays with PADs. However, these approaches still involve reagent handling related to the CRISPR reaction.[15,16] Meanwhile, Nguyen *et al.* have reported a paper-based face-mask sensor with all the reagents related to reactions pre-deposited and pre-dried on the paper substrate,[17] minimizing reagent handling by the user. However, their system has some remaining drawbacks, including counter-intuitive and qualitative turn-off signal readouts.

Due to their low cost, portability, rapidness, quantifiability, and reliability, personal glucose meters (PGMs) are widely used all over the world by diabetic patients as self-diagnostic tools for monitoring blood glucose levels.[18–20] By utilizing invertase, an enzyme converting sucrose into glucose, PGMs have been adapted to perform quantitative assays for a broad palette of non-glucose targets like small molecules,[21,22] metal ions,[23] proteins,[24,25] bacteria,[26] and nucleic acids.[27] These also already include a number of reports combining PADs with PGMs for signal detection.[22,23,26] However, these earlier studies reveal that either the squeezing of a paper or device disassembly is required to collect liquid for the final PGM measurements.

Not surprisingly, systems making use of the advantages of CRISPR/Cas have joined this list of examples for the detection

Department of Applied Chemistry, Faculty of Science and Technology, Keio University, 3-14-1 Hiyoshi, Kohoku-ku, Yokohama 223-8522, Japan.
E-mail: citterio@applc.keio.ac.jp; Tel: +81 45 566 1568

†Electronic supplementary information (ESI) available: Sequences of nucleic acids, estimated material costs to fabricate the paper-based device, evaluation of the amount of invertase immobilized on MBs, wax-printing pattern, hydrophobicity of the surface of time adjustment film, photograph of the fabricated PAD for basic evaluation, illustrations and photograph of the fully integrated device, SEM images for various pore sizes of paper and MBs, SEM images after drying MB conjugates, workability of trehalose as stabilizer for freeze-drying MB conjugates, droplet behaviour depending on orientation of the wax-printed paper surface, scheme of sample flow inside the paper substrate. See DOI: https://doi.org/10.1039/d4an00905c

of nucleic acids using PGMs.[28–31] However, these prior assays still require handling of reagents in microtubes, as well as multiple steps of operation including magnetic separation, which is against the concept of POCT. Meanwhile, Li *et al.* reported a CRISPR-mediated microfluidic biosensor with PGM readout for human immunodeficiency virus (HIV) detection.[32] While being attractive in terms of eliminating multiple manual operational steps, there remain some drawbacks, such as the cost of a 3D-printed device and magnet, reagent instability, and the requirement for reagent handling before performing the assay. Our group recently investigated the stability of CRISPR-related reagents in the dried state, including Cas12a-crRNA complex and fluorophore- and quencher-modified ssDNA on a paper platform, and these showed good storage stability up to 84 days.[33] Whereas these results confirmed the general applicability of the CRISPR/Cas12a system in POCT devices, the focus was on the most widely used fluorescent reporter signalling approaches.

In the context of these previously reported approaches, the current work realizes a CRISPR-based PAD for nucleic acid quantification with a PGM. To the best of our knowledge, this is the first report of a CRISPR/Cas-based assay being integrated into a PAD with PGM signal readout. Pre-deposition of all required reagents on a multi-layered paper device enables assays to be performed by end-users with simple operation without reagent handling, while at the same time extending the storage stability of the reagents. The developed device has a multi-layered structure consisting of three paper layers to perform the following two reactions: (1) CRISPR/Cas12a-based reaction, and (2) invertase enzymatic reaction. Application of a sample containing double-stranded target DNA (tgDNA) onto the first layer of the device activates Cas12a-crRNA complexes, which subsequently cleave invertase-conjugated ssDNA immobilized on the surface of magnetic beads (MB conjugate), resulting in the release of invertase. The released enzyme passes through a filter layer to reach the third paper layer after removing a hydrophobic film (time adjustment film) separating the first and second paper layers, while magnetic beads are retained by the filtering ability of the paper. It should be noted that in this work, magnetic beads are only used as a practical platform enabling surface modification. No magnetic component is required in the PAD, since magnetic beads are retained in the cellulosic filter layer. After reaching the third paper layer, the released invertase converts the pre-deposited sucrose to glucose, which is subsequently detected by the PGM (Fig. 1). The necessary operations by end-users are limited to sample application, removal of the time adjustment film, adding washing buffer, and taking the PGM measurement, which significantly improves the user-friendliness of the assay. Furthermore, pre-deposition of the necessary reagents could successfully extend the storage stability of the device, which is of high relevance for POCT.

Materials and methods

Materials

All the nucleic acids used in this work, including target dsDNA (tgDNA), crRNA, and ssDNA for invertase conjugation, were obtained from Integrated DNA Technologies (Singapore). The sequences are listed in Table S1.† LbCas12a was purchased from New England Biolabs, Inc. (Ipswich, MA, USA). Invertase from baker's yeast (*S. cerevisiae*) was purchased from Sigma-Aldrich (St. Louis, MO, USA). Magnetic beads (1.0 and 2.8 μm) were purchased from Thermo Fisher Scientific (Waltham, MA, USA). 3-Sulfo-*N*-succinimidyl 4-(*N*-maleimidomethyl)cyclohexane-1-carboxylate sodium salt (sulfo-SMCC) was purchased from Tokyo Chemical Industry (Tokyo, Japan). Sucrose, sodium chloride, trisodium citrate dihydrate, BSA, trehalose dihydrate, and Tween-20 were purchased from FUJIFILM Wako Pure Chemical Corporation (Osaka, Japan). Tris(2-carboxyethyl) phosphine hydrochloride (TCEP) and di-sodium hydrogen phosphate heptahydrate were purchased from Nacalai Tesque (Kyoto, Japan). Dextran (MW: 70 000) was purchased from Junsei Chemical (Tokyo, Japan). Glycine was purchased from Kanto Chemical (Tokyo, Japan). As for filter papers, Whatman Grade 1 (WF1) and Grade 4 (WF4) were purchased from GE Healthcare Life Sciences (Marlborough, MA, USA), while Advantec 5C (A5C) was obtained from Toyo Roshi, Co., Ltd (Tokyo, Japan). All filter papers were cut to A4 size before patterning. Transparent film was purchased from EPSON (Tokyo, Japan). Buffers used in this report are as follows: buffer A: 0.1 M pH 7.3 sodium phosphate buffer including 0.1 M sodium chloride; buffer B: 0.1 M pH 7.3 sodium phosphate

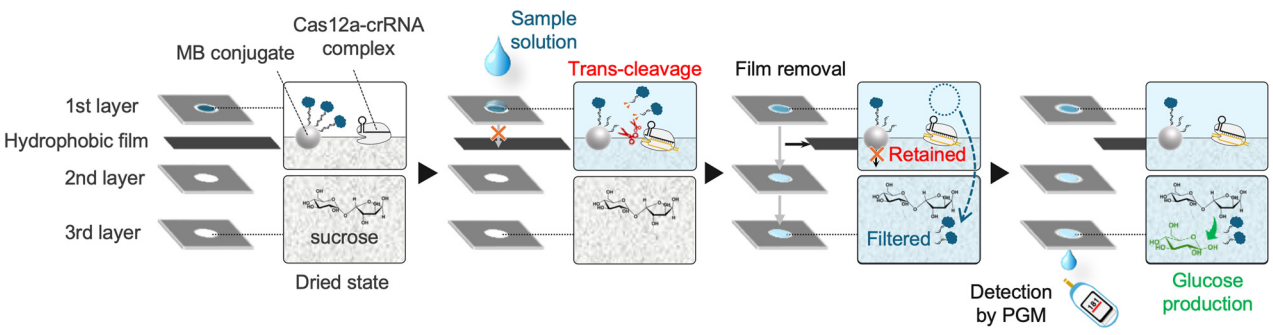

Fig. 1 Illustration of the working principle of nucleic acid quantification with a CRISPR PAD and PGM.

buffer including 0.1 M sodium chloride, and 0.01% Tween-20; buffer C: 0.1 M pH 7.3 sodium phosphate buffer including 0.1 M sodium chloride, and 0.1% BSA; buffer D: 20 mM pH 7.5 HEPES buffer including 50 mM sodium chloride, and 20 mM magnesium chloride; buffer E: 40 mM pH 7.5 HEPES buffer including 0.1 M sodium chloride, 40 mM magnesium chloride, and 0–100 g L^{-1} stabilizer (trehalose, dextran, or glycine); and buffer F: 0.1 M pH 5.6 sodium citrate buffer. All buffers were autoclaved (SP200, Yamato Scientific Co., Ltd, Tokyo, Japan) at 180 °C and stored at 4 °C for further use.

Synthesis of invertase-conjugated ssDNA immobilized on magnetic beads

The invertase-conjugated ssDNA immobilized on magnetic beads (MB conjugate) was synthesized by referring to previously reported methods with slight modifications.[21,28,30] Specifically, 1 mg of sulfo-SMCC was first added to 400 μL of 10 mg mL^{-1} invertase solution in buffer A, followed by incubation on a rotator for 60 min. The mixture was then centrifuged twice to remove solid sulfo-SMCC and purified by using Vivaspin Turbo 4 (MWCO: 100 kDa) ultrafiltration tubes 6 times with buffer A. The disulfide-modified ssDNA was reduced before use by either of the following methods: 15 μL of 0.1 M TCEP in buffer A was added to 15 μL of 1 mM ssDNA in autoclaved water, or directly to 15 nmoles of freeze-dried ssDNA, followed by incubation for 60 min. Activated invertase supernatant obtained after purification was then added to the reduced ssDNA solution, and the mixture was incubated on the rotator for 120 min. After further purification using Vivaspin Turbo 4 (MWCO: 100 kDa) ultrafiltration tubes 6 times with buffer A, 100 μL of 10 mg mL^{-1} streptavidin-coated magnetic beads (MBs, diameter = 1.0 or 2.8 μm) in buffer B was added to the supernatant obtained after purification, followed by incubation on the rotator for 60 min. Lastly, the mixture was washed with buffer C 6 times and buffer D 3 times, using magnetic separation. The immobilization of invertase-conjugated ssDNA on MBs was confirmed by detecting glucose as the product of the invertase enzymatic reaction using the PGM (Fig. S1†).

Fabrication of the PAD for basic evaluation

Paper spot patterning was achieved by a wax-printing method.[34] Specifically, the pattern designed in Adobe Illustrator CC software (Fig. S2†) was printed by a black solid ink wax-printer (ColorQube 8580, Xerox, Norwalk, USA). Wax-printed filter papers were then heated on a hot plate (NHS-450 ND, Nissin Rika, Chiba, Japan) at 150 °C for 2.5 min (WF1 and WF4) or 3 min (A5C). Subsequently, the patterned filter papers were cut in a way that three paper spots (diameters of each spot from the 1st to 3rd layer were 5.5, 5.0 and 5.0 mm before heating) were included in one row (Fig. S2†). For paper blocking, 10 μL of BSA (various concentrations as specifically indicated) in autoclaved water was dropped onto the paper spots of the 1st and 2nd paper layer and dried at 37 °C for 120 min. The time adjustment film was obtained by modifying the surface of a transparent film (A4 size, 100 μm thickness, Epson, Tokyo, Japan) with black toner deposited using a laser-printer (DocuCentreIV C2263, Xerox, Norwalk, USA), which rendered its surface hydrophobic (Fig. S3†) and prevented liquid leakage. Subsequently, the toner-modified film was cut into rectangular shapes (25 mm × 7.5 mm) using a Silhouette CAMEO 3 autocutter (Silhouette, Lindon, UT, USA). Finally, the wax-patterned and cut paper strip was folded, "origami-style", so that the layer with the largest spot diameter was at the top of the device, the time adjustment film was inserted between the 1st and 2nd paper layer (toner-modified surface facing upwards) and all layers were held together using four clips (Fig. S4†).

Investigation of filtering ability

A mixture containing 100 nM Cas12a and 200 nM crRNA (Cas12a/crRNA) in buffer D was pre-incubated for 15–30 min. Afterwards, 3 μL of the pre-incubated solution, 1 μL of 20 mg mL^{-1} MB conjugate in buffer D, 4 μL of buffer D, and 2 μL of 0 or 100 nM tgDNA in autoclaved water were dropped on the paper spot of the 1st layer of the above-described device. After incubation for 60 min in a humid environment, achieved by placing devices in a closed container lined with wetted kitchen paper towel, the time adjustment film was removed, and the device was left for a further 5 min for liquid penetration into the lower layers. Subsequently, the device was unfolded, and 5 μL of sucrose solution (3.75 μL of 1 M sucrose in autoclaved water, 0.75 μL of buffer F, and 0.5 μL of autoclaved water) was dropped on the paper spots of the 2nd and 3rd layers, followed by additional incubation for 60 min in a humid environment. Lastly, the concentration of glucose produced on the 2nd and 3rd layers was measured by using the PGM. SEM images (FE-SEM-H2, Hitachi, Tokyo) of paper layers were obtained without the addition of sucrose after osmium coating (HPC-20, Vacuum Device, Ibaraki, Japan).

Consideration of drying methods and the necessity of stabilizers

3 μL of pre-incubated (15–30 min) Cas12a/crRNA mixture and 1 μL of 20 mg mL^{-1} of MB conjugate in buffer E were dropped on the paper spot of the 1st layer of the device, followed by drying for 60 min either at 37 °C or by freeze drying (snap freezing using liquid nitrogen followed by applying a vacuum).

After applying 10 μL of 0 or 100 nM tgDNA in autoclaved water onto the device, the assay was carried out as described in the previous section.

Fabrication of the fully integrated device and its assay use

Wax-printed paper (diameters of each spot from the 1st to 3rd layer were 5.5, 5.0, and 5.0 mm before heating) was prepared as mentioned above, with the difference being of cutting each layer into a separate piece of paper instead of using the origami strip-folding approach. At the same time of paper blocking of the 1st and 2nd layers using 10 μL of BSA in autoclaved water, 3 μL of sucrose solution (2.25 μL of 1 M sucrose in autoclaved water, 0.45 μL of buffer E, and 0.3 μL of autoclaved water) was dropped on the paper spot of the 3rd layer,

followed by drying at 37 °C for 120 min. Subsequently, the device was assembled by stacking the paper layers with a time adjustment film placed in between the 1st and 2nd layers, and double-sided tape (90 μm thickness, Nichiban, Tokyo, Japan) in between the 2nd and 3rd layers in a "sandwiched style" as illustrated in Fig. S5A.† The double-sided tape was cut using the autocutter (16 mm × 16 mm, hole diameter = 3.5 mm). Afterwards, the sandwiched layers were fixed onto a lamination film (A4 size, 100 μm thickness, made of polyethylene terephthalate and polyvinyl alcohol as a thermoplastic adhesive, Jointex, Tokyo, Japan) using tape. To provide a liquid inlet and outlet, a hole (φ = 7.0 mm) was cut into the lamination film using the autocutter before fixing the device. Subsequently, the device was passed through a hot laminator (Office Pro A3, Leitz, Oberkochen, Germany). For additional fixation, the device was stapled twice as shown in Fig. S5B.† As a final step, the adhesive between the time adjustment film and lamination film was removed using a thin needle to facilitate removal of the time adjustment film during the assay. Then, 3 μL of pre-incubated Cas12a-crRNA and 1 μL of 20 mg mL^{-1} MB conjugates in buffer E were dropped onto the top paper layer spot of the device and freeze-dried for 60 min (snap freezing using liquid nitrogen followed by applying vacuum conditions).

Assays using the above-prepared devices were performed as follows: first, 10 μL of tgDNA in autoclaved water was dropped onto the sample inlet, followed by incubation for 60 min in a humid environment. After removing the time adjustment film, 10 μL of buffer D was applied as washing buffer. Following additional incubation for 60 min in a humid environment, the concentration of produced glucose in the droplet formed on the back side of the device (below the 3rd layer) was measured using the PGM.

Storage stability test

Fully integrated devices prepared as mentioned above were stored at −20 °C in aluminium-coated pouches containing a silica gel desiccant until further use. Assays were then carried out as mentioned above.

Results and discussion

Filtering ability for magnetic bead retention

To enhance the tgDNA-dependent signal over the background, it highly important to retain magnetic beads with invertase-conjugated ssDNA on the inlet paper layer (1st layer) while enabling passage of invertase released by trans-cleavage to the 3rd layer with pre-deposited sucrose. To experimentally confirm the filtering ability, the presence of invertase in the 2nd and 3rd paper layers was evaluated indirectly both in the absence and presence of tgDNA by measuring the glucose levels in these layers using the PGM after device unfolding and sucrose addition. Devices made from three types of filter papers having different pore size (A5C: 1.0 μm, WF1: 10.8 μm, WF4: 22–25 μm) and MBs with two different diameters (1.0 μm and 2.8 μm) were used. As Fig. 2 shows, significant signal differences between blank samples (0 nM tgDNA) and tgDNA-containing samples were observed in all cases, which successfully demonstrates the retention of magnetic beads with non-cleaved invertase on the top paper layer. As theoretically expected, the blank signal on both the 2nd and 3rd layers increased in the order of the filter paper particle retention size, due to failure in retaining MBs on the top layer, being lowest for devices made of A5C paper with the smallest pore size. Furthermore, comparing the results obtained with smaller (Fig. 2A) and larger MBs (Fig. 2B), the overall blank signals were larger in the case using the smaller 1.0 μm diameter beads. The retention of MBs depending on paper pore and MB size was also substantiated by SEM images (Fig. S6†), with the number of MBs on each layer qualitatively indicating similar trends as the blank signals observed through quantification of invertase-generated glucose. Higher blank signals (Fig. 2) correspond to a larger number of MBs passing through the top paper layer of the device to lower layers (Fig. S6†). These experiments also revealed overall higher glucose signals for tgDNA-positive samples, when using smaller sized MBs, attributed to their 2.8 times larger surface area compared to their larger counterparts. Considering these results, the A5C

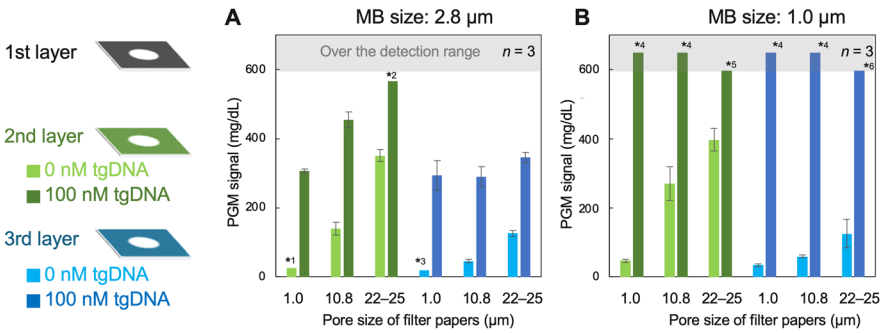

Fig. 2 Dependence of PGM signals detected on the 2nd and 3rd paper layers on MB diameter (A: 2.8 μm and B: 1.0 μm) and pore size of filter papers (1.0 μm: A5C, 10.8 μm: WF1, 20–25 μm: WF4) in the absence (0 nM) or presence (100 nM) of tgDNA; error bars represent the mean values ± 1σ (n = 3). Results presented without error bars include signals below or above the detection range (20–600 mg dL^{-1}) of the used PGM (*1: <20, 36 and 22 mg dL^{-1}, *2: 579, >600 and 518 mg dL^{-1}, *3: <20, 20 and 20 mg dL^{-1}, *4: all >600 mg dL^{-1}, *5: >600, >600 and 587 mg dL^{-1}, *6: >600, >600 and 591 mg dL^{-1}).

filter paper with 1.0 μm pore size and the 1.0 μm diameter MBs were selected for further experiments.

Consideration of reagent drying methods and the necessity of stabilizers

The Cas12a/crRNA complex and MB conjugates require careful consideration for drying due to their enzyme content. To investigate their drying tolerance, two drying methods were first compared: heat-drying and freeze-drying. As Fig. 3A shows, a tgDNA-dependent signal difference was confirmed after drying by either method, proving the retained enzymatic activity of both the Cas12a/crRNA complex and invertase. However, the blank signal in the case of the freeze-drying method was significantly decreased compared to that after heat-drying, which is mainly attributed to the different characteristics of the two drying methods. While MBs in the wet paper are mobile during gradual water evaporation at 37 °C, this mobility is prevented by the immediate snap freezing in the freeze-drying procedure, resulting in the prevention of penetration of MB conjugates into the depth of the paper substrate. This hypothesis is supported by the SEM images recorded at the top and bottom sides of paper substrates after drying (Fig. S7†), where the appearance of MBs on the back side was only confirmed after heat-drying. Therefore, the freeze-drying approach was selected for further investigations.

Subsequently, the necessity of using protective stabilizer molecules was investigated. It is generally said that addition of stabilizers is an important factor to extend the stability of proteins, since most proteins dried in their absence cannot survive desiccation.[35] There are many possible candidates for stabilizers including osmolytes, sugars, polymers, and proteins. However, their efficiency differs between experimental conditions.[36] Several previous works have reported on the preserved activity of Cas complexes freeze-dried in the presence of BSA, trehalose, sucrose, dextran, or glycine.[37,38] Based on these facts, the workability of trehalose, dextran, and glycine as stabilizers for Cas12a/crRNA complexes and MB conjugates freeze-dried on filter paper substrates was compared. Unexpectedly, the results shown in Fig. 3B indicate that tgDNA-positive signals were not significantly increased by adding stabilizers, which can be explained by the presence of BSA used for paper blocking working as a stabilizer.[33] However, trehalose most effectively suppressed the blank signal compared to drying without stabilizers or with dextran and glycine. This positive influence of trehalose on the background signal was also confirmed in the case of MB conjugates being freeze-dried in microtubes (Fig. S8†). This suggests that the blank signal suppression observed on the paper platform due to the presence of trehalose during drying is not related to the prevention of MB conjugate leakage through the paper layers, but likely to the stabilization of the invertase–MB conjugates in the dried state. It has been reported that the binding between biotin and streptavidin is disrupted when dried, and that this disruption can be prevented by adding trehalose to the system before drying.[39] Since the invertase-conjugated ssDNA is anchored to the MBs through the streptavidin–biotin interaction, any disruption of this linkage results in the tgDNA-independent release of invertase and, consequently, an increase in the blank signal. For these reasons, freeze-drying in presence of trehalose was selected as the optimal preservation method of Cas12a/crRNA complexes and MB conjugates.

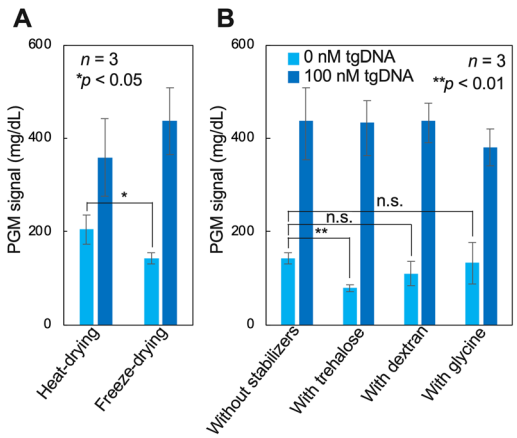

Fig. 3 (A) Comparison of tgDNA-dependent PGM signals after heat-drying or freeze-drying of Cas12a/crRNA complexes and MB conjugates; (B) PGM signals depending on the presence and type of stabilizers in buffer E (40 g L^{-1} trehalose, dextran, or glycine) during freeze-drying of Cas12a/crRNA complexes and MB conjugates; A5C was used as a paper substrate; concentration of BSA for blocking was 1 wt%; n.s., not significant with $p > 0.05$; error bars represent the mean values ± 1σ ($n = 3$).

Development of a fully integrated device

The handling of devices used for the above-described basic evaluation experiments involved an unfolding step to add sucrose solution. To realize a fully integrated paper device for "sample-in–answer-out" assays, a design including pre-deposited sucrose was evaluated. To enable signal detection by the PGM without the requirement for additional user engagement, as in earlier works,[22,23,26] it is necessary for a liquid droplet to form on the back side of the device after the application of sample and washing buffer. Through various screening investigations, it was found that droplet formation occurred only when the multilayer paper devices were assembled with the wax-printed face of each paper layer facing upwards (Fig. S9†). This paper orientation-dependence of the vertical sample liquid flow can be explained by the wax-penetration behaviour during the paper-patterning step, resulting in a conical frustum shape.[34] As a result, a vertical downward force is only created when the wax-printed paper surface is oriented upwards (Fig. S10†).

PGM assay optimization

For the current assay approach, it is highly important to efficiently transport invertase released from the surface of the MB conjugates through tgDNA-induced trans-cleavage at the top paper layer to the bottom layer with pre-deposited sucrose. Since proteins are generally easily adsorbed on paper sub-

strates, surface blocking is required. BSA is among the preferred well-known blocking reagents, due to its low cost and limited steric hindrance of specifically binding proteins.[40] With increasing concentration of BSA in the blocking solution, enhanced tgDNA-dependent signals were observed (Fig. 4A), confirming the passage of trans-cleaved invertase through the paper layers. At BSA concentrations of 5% or higher (data not shown), the applied blocking solution did not dry homogeneously, thus 2.5% of BSA was ultimately applied for paper blocking. Subsequently, the concentration of trehalose stabilizer was optimized using the fully integrated device. As a result, blank signals were most efficiently suppressed at 50 g L^{-1} trehalose added during freeze-drying, with no further improvement at higher concentrations (Fig. 4B). Lastly, the dependence of the PGM signal on the reaction times of the double enzymatic reaction (CRISPR and invertase) was investigated. As shown in Fig. 4C, the signals at lower tgDNA levels of 0.1 and 1 nM were particularly increased by extending the CRISPR reaction time, with significant tgDNA concentration-dependent signals obtained after 60 min. These time-dependent signal-change trends for the CRISPR reaction were consistent with previous reports,[41,42] suggesting the successful working of the CRISPR/Cas12a system on the developed paper device. On the contrary, in differing from the time-dependence of the CRISPR reaction (ssDNA-cleavage), there was a linear relationship between the invertase reaction time (sucrose to glucose conversion) and the PGM signals (Fig. 4D), the trend of which again being similar to previously reported assay systems relying on PGMs for non-glucose target detection.[32,43]

Analytical performance of the assay with the fully integrated device

The analytical performance of the fully integrated device with the optimized parameters was investigated. For proof-of-concept, double-stranded human papilloma virus (HPV) DNA of 43 bp length was selected as a model. As Fig. 5A indicates, the logarithmic concentration–response curve followed a sigmoidal function (R^2 = 0.993), fitted with the following Hill equation:

$$y = 85.7 + \frac{272.3x^{0.917}}{1.09 + x^{0.917}}$$

indicating the feasibility of tgDNA quantification with the developed device. The limit of detection estimated according to the 3σ method was 57 pM, which is comparable to other reported amplification-free POC CRISPR-based assays for detecting nucleic acids.[8,44–46]

Finally, the storage stability (−20 °C in a freezer) of the fully integrated device was investigated. As Fig. 5B shows, the orig-

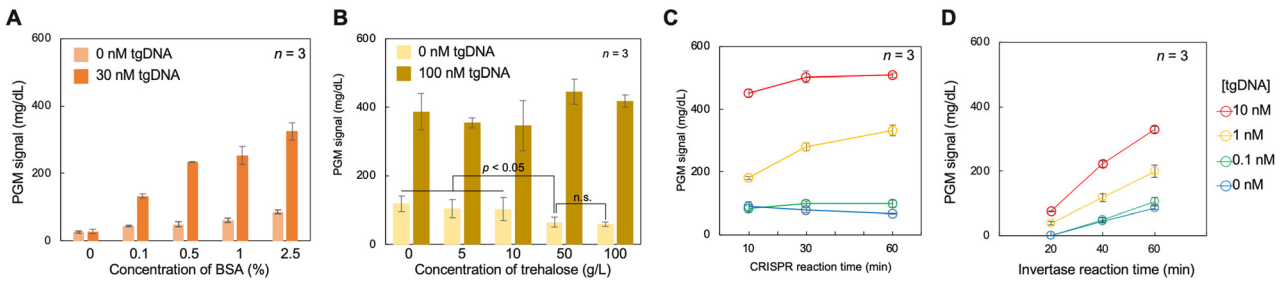

Fig. 4 PGM signal intensities depending on (A) the concentration of BSA (10 μL applied to the 1st and 2nd paper layers) used for paper blocking and (B) the concentration of trehalose applied during freeze-drying. (C) The relationship between CRISPR reaction time and PGM signal with 60 min of invertase reaction time. (D) The relationship between invertase reaction time and PGM signal with 60 min of CRISPR reaction time; n.s., not significant with $p > 0.05$; error bars represent the mean values ± 1σ (n = 3); the result without an error bar in (D) includes signals below the detection range of the PGM (<20, <20 and 20 mg dL^{-1}).

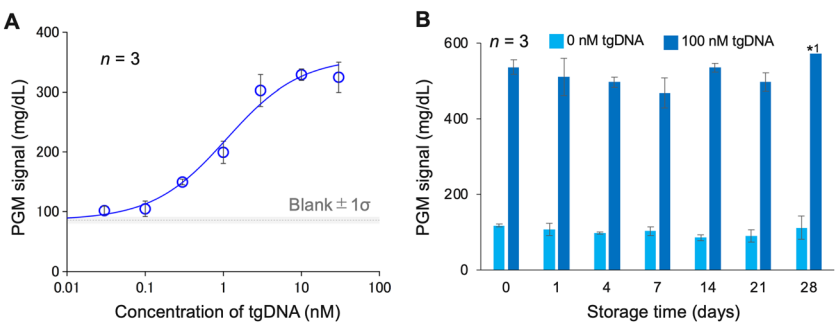

Fig. 5 (A) Relationship between tgDNA concentration and PGM signal after 60 min of CRISPR reaction time and another 60 min of invertase reaction time. (B) Storage stability of the fully integrated device at −20 °C; error bars represent the mean values ± 1σ (n = 3); the result without an error bar includes signals above the detection range of the PGM (521, 596 and >600 mg dL^{-1}).

inal tgDNA-positive PGM signal was maintained throughout the 28 days of storage, suggesting no deterioration of the enzymatic activities of the Cas12a/crRNA complex and invertase. In addition, no increase in the blank signal was observed over time, proving the successful stable immobilization of invertase on MBs.

Although providing only a very rough estimate, costs of the materials required to fabricate the fully integrated device are summarized (Table S2†). It can be stated that the material costs of the paper-based components including all the pre-deposited reagents are of the same order of magnitude as the market price of the commercialized single-use PGM electrode. However, it should be noted that the latter includes labour and manufacturing costs, which are not included in the case of the former.

Conclusions

The current work established a fully integrated paper-based CRISPR-assisted nucleic acid quantification device with signal detection using a PGM. This system has been achieved by separation of MBs and released invertase by the inherent filtering ability of paper substrates without a requirement for any additional equipment. Three factors contributed to the successful realization of this system: (1) introduction of a hydrophobic film to control the time for the two enzymatic reaction steps; (2) on-device liquid droplet formation for direct glucose meter measurements without any additional operational steps; and (3) stabilizing the MB conjugates in the dry state. The pre-deposition of all required reagents onto the paper-based device contributed to simplified operation of an assay, which conventionally required magnetic separation and multiple-reagent handling steps. By utilizing widely available commercial PGMs for the signal readout, quantitative assay results are obtained without sacrificing user-friendliness. Furthermore, pre-deposition and drying of reagents resulted in extended storage stability, which is generally difficult to achieve for solution-state reagents. However, it must be mentioned that the current study only demonstrates the feasibility of nucleic acid quantification by a paper-based CRISPR/Cas assay with PGM signal readout. As in previously reported approaches relying on the detection of non-glucose targets using PGMs, either differential measurements or the removal of glucose from the sample, for example through reaction with glucose oxidase, is required for application toward clinical samples containing endogenous glucose.[19,47] Yet, we still believe that the current work represents a first important step towards user-friendly and quantitative "sample-in–answer-out" POCT for nucleic acids.

Author contributions

Yohei Tanifuji: conceptualization, methodology, investigation, data curation, formal analysis, writing – original draft. Guodong Tong: conceptualization, methodology, investigation, supervision. Yuki Hiruta: validation, writing – review & editing, supervision, funding acquisition. Daniel Citterio: conceptualization, methodology, validation, writing – review & editing, supervision, project administration, funding acquisition.

Data availability

Data created and analysed in this study are included in the article and the ESI.† Raw data supporting the findings of this study are available from the corresponding author upon reasonable request.

Conflicts of interest

There are no conflicts to declare.

Acknowledgements

The authors acknowledge financial support *via* a Grant-in-Aid for Scientific Research (B) (grant no. 22H02109) from the Japan Society for the Promotion of Science (JSPS), and the Nakatani Foundation for Advancement of Measuring Technologies in Biomedical Engineering Grant Program for Research Study to D.C.

References

1 J. E. Van Dongen, J. T. W. Berendsen, R. D. M. Steenbergen, R. M. F. Wolthuis, J. C. T. Eijkel and L. I. Segerink, *Biosens. Bioelectron.*, 2020, **166**, 112445.
2 M. M. Kaminski, O. O. Abudayyeh, J. S. Gootenberg, F. Zhang and J. J. Collins, *Nat. Biomed. Eng.*, 2021, **5**, 643–656.
3 A. S. Avaro and J. G. Santiago, *Lab Chip*, 2023, **23**, 938–963.
4 M. Bao, Q. Chen, Z. Xu, E. C. Jensen, C. Liu, J. T. Waitkus, X. Yuan, Q. He, P. Qin and K. Du, *ACS Sens.*, 2021, **6**, 2497–2522.
5 C. Yuan, T. Tian, J. Sun, M. Hu, X. Wang, E. Xiong, M. Cheng, Y. Bao, W. Lin, J. Jiang, C. Yang, Q. Chen, H. Zhang, H. Wang, X. Wang, X. Deng, X. Liao, Y. Liu, Z. Wang, G. Zhang and X. Zhou, *Anal. Chem.*, 2020, **92**, 4029–4037.
6 M. Broto, M. M. Kaminski, C. Adrianus, N. Kim, R. Greensmith, S. Dissanayake-Perera, A. J. Schubert, X. Tan, H. Kim, A. S. Dighe, J. J. Collins and M. M. Stevens, *Nat. Nanotechnol.*, 2022, **17**, 1120–1126.
7 S. Gong, X. Wang, P. Zhou, W. Pan, N. Li and B. Tang, *Anal. Chem.*, 2022, **94**, 15839–15846.
8 J. Ki, H.-K. Na, S. W. Yoon, V. P. Le, T. G. Lee and E.-K. Lim, *ACS Sens.*, 2022, **7**, 3940–3946.
9 J. H. Choi, J. Lim, M. Shin, S. H. Paek and J. W. Choi, *Nano Lett.*, 2021, **21**, 693–699.

10 J. Yan, Z. Xu, H. Zhou, T. Li, X. Du, R. Hu, J. Zhu, G. Ou, Y. Li and Y. Yang, *Anal. Chem.*, 2022, **94**, 16481–16490.
11 J. P. Broughton, X. Deng, G. Yu, C. L. Fasching, V. Servellita, J. Singh, X. Miao, J. A. Streithorst, A. Granados, A. Sotomayor-Gonzalez, K. Zorn, A. Gopez, E. Hsu, W. Gu, S. Miller, C.-Y. Pan, H. Guevara, D. A. Wadford, J. S. Chen and C. Y. Chiu, *Nat. Biotechnol.*, 2020, **38**, 870–874.
12 J. S. Gootenberg, O. O. Abudayyeh, J. W. Lee, P. Essletzbichler, A. J. Dy, J. Joung, V. Verdine, N. Donghia, N. M. Daringer and C. A. Freije, *Science*, 2017, **356**, 438–442.
13 Anushka, A. Bandopadhyay and P. K. Das, *Eur. Phys. J.: Spec. Top.*, 2023, **232**, 781–815.
14 K. Yamada, H. Shibata, K. Suzuki and D. Citterio, *Lab Chip*, 2017, **17**, 1206–1249.
15 H. Cao, K. Mao, F. Ran, P. Xu, Y. Zhao, X. Zhang, H. Zhou, Z. Yang, H. Zhang and G. Jiang, *Environ. Sci. Technol.*, 2022, **56**, 13245–13253.
16 D. Huang, D. Ni, M. Fang, Z. Shi and Z. Xu, *Anal. Chem.*, 2021, **93**, 16965–16973.
17 P. Q. Nguyen, L. R. Soenksen, N. M. Donghia, N. M. Angenent-Mari, H. De Puig, A. Huang, R. Lee, S. Slomovic, T. Galbersanini, G. Lansberry, H. M. Sallum, E. M. Zhao, J. B. Niemi and J. J. Collins, *Nat. Biotechnol.*, 2021, **39**, 1366–1374.
18 A. Heller and B. Feldman, *Chem. Rev.*, 2008, **108**, 2482–2505.
19 F. Lisi, J. R. Peterson and J. J. Gooding, *Biosens. Bioelectron.*, 2020, **148**, 111835.
20 S. Zhang, S. Li, R. Yan, Z. Zhou, Y. Wu and Y. Lu, *Curr. Anal. Chem.*, 2022, **18**, 705–722.
21 Y. Xiang and Y. Lu, *Nat. Chem.*, 2011, **3**, 697–703.
22 J. Zhang, Z. Shen, Y. Xiang and Y. Lu, *ACS Sens.*, 2016, **1**, 1091–1096.
23 W. Xiao, Y. Gao, Y. Zhang, J. Li, Z. Liu, J. Nie and J. Li, *Biosens. Bioelectron.*, 2019, **137**, 154–160.
24 Y. Xiang and Y. Lu, *Anal. Chem.*, 2012, **84**, 4174–4178.
25 F. Hossain, Q. Shen, N. Balasuriya, J. L. M. Law, M. Logan, M. Houghton, D. L. Tyrrell, M. A. Joyce and M. J. Serpe, *Anal. Chem.*, 2023, **95**, 7620–7629.
26 H. Huang, G. Zhao and W. Dou, *Biosens. Bioelectron.*, 2018, **107**, 266–271.
27 X. Xue-Tao, L. Kai-Yi and Z. Jia-Ying, *Analyst*, 2014, **139**, 4982–4986.
28 B. Fang, Z. Jia, C. Liu, K. Tu, M. Zhang and L. Zhang, *Talanta*, 2022, **249**, 123657.
29 R. Liu, Y. Hu, Y. He, T. Lan and J. Zhang, *Chem. Sci.*, 2021, **12**, 9022–9030.
30 D. Huang, Z. Shi, J. Qian, K. Bi, M. Fang and Z. Xu, *Biotechnol. Bioeng.*, 2021, **118**, 1568–1577.
31 S. Gong, J. Li, W. Pan, N. Li and B. Tang, *Anal. Chem.*, 2021, **93**, 10719–10726.
32 Z. Li, N. Uno, X. Ding, L. Avery, D. Banach and C. Liu, *ACS Nano*, 2023, **17**, 3966–3975.
33 Y. Tanifuji, H. Suzuki, G. Tong, Y. Hiruta and D. Citterio, *Anal. Methods*, 2024, **16**, 4143–4149.
34 E. Carrilho, A. W. Martinez and G. M. Whitesides, *Anal. Chem.*, 2009, **81**, 7091–7095.
35 J. A. Brom, R. G. Petrikis and G. J. Pielak, *Biochemistry*, 2023, **62**, 1044–1052.
36 S. Piszkiewicz and G. J. Pielak, *Biochemistry*, 2019, **58**, 3825–3833.
37 Y. Wang, H. Chen, H. Gao, H. Wei, Y. Wang, K. Mu, L. Liu, E. Dai, Z. Rong and S. Wang, *Biosens. Bioelectron.*, 2023, **229**, 115238.
38 G. A. Rybnicky, R. A. Dixon, R. M. Kuhn, A. S. Karim and M. C. Jewett, *ACS Synth. Biol.*, 2022, **11**, 835–842.
39 N. Xia, J. S. Shumaker-Parry, M. H. Zareie, C. T. Campbell and D. G. Castner, *Langmuir*, 2004, **20**, 3710–3716.
40 Y. L. Jeyachandran, J. A. Mielczarski, E. Mielczarski and B. Rai, *J. Colloid Interface Sci.*, 2010, **341**, 136–142.
41 D. A. Huyke, A. Ramachandran, V. I. Bashkirov, E. K. Kotseroglou, T. Kotseroglou and J. G. Santiago, *Anal. Chem.*, 2022, **94**, 9826–9834.
42 Y. He, S. Shao and J. Chen, *ACS Sens.*, 2023, **8**, 4478–4483.
43 Z. Jia, Z. Li and C. Liu, *Sens. Actuators, B*, 2023, **390**, 133994.
44 M. Zeng, Y. Ke, Z. Zhuang, C. Qin, L. Y. Li, G. Sheng, Z. Li, H. Meng and X. Ding, *Anal. Chem.*, 2022, **94**, 10805–10812.
45 Z. Ji, B. Zhou, Z. Shang, S. Liu, X. Li, X. Zhang and B. Li, *Anal. Chem.*, 2023, **95**, 10580–10587.
46 N. Shao, X. Han, Y. Song, P. Zhang and L. Qin, *Anal. Chem.*, 2019, **91**, 12384–12391.
47 L. Yan, Z. Zhu, Y. Zou, Y. Huang, D. Liu, S. Jia, D. Xu, M. Wu, Y. Zhou, S. Zhou and C. J. Yang, *J. Am. Chem. Soc.*, 2013, **135**, 3748–3751.